

New Technique for Investigating Noncrystalline Structures: Fourier Analysis of the Extended X-Ray–Absorption Fine Structure*

Dale E. Sayers† and Edward A. Stern‡

Department of Physics, University of Washington, Seattle, Washington 98105

and

Farrel W. Lytle

Boeing Scientific Research Laboratories, Seattle, Washington 98124

(Received 16 July 1971)

We have applied Fourier analysis to our point-scattering theory of x-ray absorption fine structure to invert experimental data formally into a radial structure function with determinable structural parameters of distance from the absorbing atom, number of atoms, and widths of coordination shells. The technique is illustrated with a comparison of evaporated and crystalline Ge. We find that the first and second neighbors in amorphous Ge are at the crystalline distance within the accuracy of measurement (1%).

Physicists have been tantalized for forty years¹ by the structurally sensitive extended x-ray absorption fine structure (EXAFS) or Kronig structure which appears on the high-energy side of x-ray absorption edges. Recently, we reported a point-scattering theory of K x-ray absorption fine structure² which gave excellent agreement with experimental structure. In this Letter we show that the point-scattering theory can be used to invert formally the experimental EXAFS data to obtain a radial structure function containing interatomic distances, number of atoms, and widths of coordination shells in the absorbing material. Amorphous and crystalline Ge are compared to illustrate the technique.

EXAFS arises from oscillations in the photoelectric cross section due to scattering of the ejected photoelectron by atoms surrounding the absorbing atom. Our theory describes this surrounding atomic array in terms of a system of point scatterers. The total photoelectron wave function, including scattering, is calculated from scattering theory and used to calculate the dipole transition matrix element of which $\chi(k)$, the oscillatory part, is retained.² The final expression for the EXAFS is

$$\chi(k) = -kf(k)\sum_j [N_j \exp(-\gamma r_j)/r_j^2] \exp(-\sigma_j^2 k^2/2) \sin[2kr_j + 2\eta(k)], \quad (1)$$

where $k = 2\pi/\lambda$ is the photoelectron wave vector, $f(k)$ is the usual electron scattering factor³ (i.e., the Fourier transform of the scattering potential), r_j is the distance from the absorbing atom to the j th coordination shell, N_j is the number of atoms at r_j , $\exp(-\gamma r_j)$ is a photoelectron scattering range term similar in form to that of Shiraiwa, Ishimura, and Sawada,⁴ and $\eta(k)$ is the phase shift of the photoelectron caused by the potential of the absorbing atom. This result is similar to earlier theories¹; however, its basis in an array of point scatterers is more realistic and flexible for calculating EXAFS in any atomic environment.

Equation (1) differs from our previous result in that the temperature factor $\exp(-\sigma_j^2 k^2/2)$ is a general Debye form where σ_j^2 is the mean square amplitude of the relative displacement of the atoms in the j th shell from the absorbing atom including both thermal and disorder contributions.⁵ Also, we have retained only the dominant term of Eq. (32) in Ref. 2. The spectra calculated from this simplified expression have changes in peak positions of less than 1 eV and changes in amplitude of less than 2% from the spectra calculated with the complete equation.²

Since EXAFS can be accounted for by a simple sum of damped sine waves, we formally invert the data in the following way. If Eq. (1) is rewritten

$$-\chi(k)k^{-1}f(k)^{-1} = \sum_j [N_j \exp(-\gamma r_j)/r_j^2] \exp(-\sigma_j^2 k^2/2) \sin[2kr_j + 2\eta(k)], \quad (2)$$

then taking the Fourier transform of this equation we obtain

$$\begin{aligned} \varphi(r) &= -(2/\pi)^{1/2} \int_0^\infty \chi(k)k^{-1}f(k)^{-1} \sin[2kr + 2\eta(k)] dk \\ &= \frac{1}{2} \sum_j [N_j \exp(-\gamma r_j)/r_j^2 \sigma_j] \exp[-2(r-r_j)^2/\sigma_j^2] + \Delta(r). \end{aligned} \quad (3)$$

Here $\Delta(r)$ is a term which is in practice very much smaller than the rest of the expression and it will be neglected from now on.

The right-hand side of Eq. (3) is the structure-related function $\varphi(r)$ obtained from the point-scattering theory. It shows that the transform of the experimental data is a sum of normalized Gaussian curves whose amplitudes are

$$A_j = N_j \exp(-\gamma r_j) / 2r_j^2 \sigma_j. \quad (4)$$

From the peak position, amplitude, and width of the Gaussian, information about the number of atoms and the magnitude of their distribution about r_j may be determined. In order to obtain complete information about the number of atoms and their disorder smearing, other information is needed. First, the width of the Gaussian contains both structural and thermal components. Assuming that both components are independent of one another, we separate their contributions by

$$\sigma_{\text{tot}}^2 = \sigma_T^2 + \sigma_D^2, \quad (5)$$

where T and D indicate thermal and disorder broadening, respectively. To evaluate σ_D separately we must either calculate σ_T from theory which is not available for amorphous materials, or, since EXAFS has been shown to be temperature dependent,⁶⁻⁸ we may measure EXAFS at several temperatures and fit the variations in width to a Debye function and thus obtain the thermal widths. Another method is to compare the data from amorphous and crystalline polymorphs and assume that the crystalline widths are entirely thermal in origin and that the amorphous widths have the same temperature dependence because of a similar short-range structure; then

$$\sigma_D^2(A) = \sigma_{\text{tot}}^2(A) - \sigma_{\text{tot}}^2(C), \quad (6)$$

where A and C stand for the amorphous and crystalline case. In a typical experiment there are also contributions to the width because of an instrumental broadening and from finite Fourier termination. The Fourier termination has been discussed by Warren⁹ and gives a broadening of

$$\Delta r = 3.8/k_m \quad (7)$$

at half-maximum. For our data $k_m \sim 20$ and $\Delta r = 0.19 \text{ \AA}$. These broadenings are difficult to calculate but may be subtracted exactly if all the experimental conditions for the amorphous and crystalline data are the same using the full observed width including termination broadening in $\sigma_{\text{tot}}(C)$ of Eq. (6).

We have described previously^{2,10} the experimental apparatus consisting of a single-crystal x-ray spectrometer operated in a stepping mode ($\Delta 2\theta = 0.005^\circ$; $\Delta eV \sim 2$) measuring the x-ray intensity with the absorber in (I) and out (I_0) of the x-ray beam. The electronic and mechanical stability of the system were such that a precision of 0.3% (this corresponds to 10^5 photons recorded for each I and I_0 at each step) was attainable.

Improved statistics (0.1%) were obtained by combining several data runs (usually about ten) on each sample. These statistics were necessary in order to resolve the EXAFS signal to $\sim 1000 \text{ eV}$. The absorber was cooled to 77.4°K in a cryostat¹⁰ (absorber material sandwiched between aluminum foil) to reduce thermal smearing of the EXAFS peaks. The crystalline Ge was prepared from a fine powder by casting in Duco cement. The amorphous Ge specimens were prepared by evaporation from a tungsten boat onto 1-mil Mylar or aluminum foil in a vacuum better than 5×10^{-6} Torr. During deposition substrate temperatures rose to $25\text{--}50^\circ\text{C}$ due to radiant heating. The thickness of the foils was approximately $1 \mu\text{m}$; six layers were used to obtain the EXAFS spectra. These samples were also analyzed by x-ray diffraction, electron diffraction and microscopy, and differential scanning calorimetry. The structural investigations showed diffraction patterns with two diffuse rings, $4\pi \sin\theta/\lambda = 1.81$ and 3.22 \AA^{-1} . Application of the Scherrer formula to the linewidth gave an apparent domain size of approximately 40 \AA .¹¹ Microscopic investigations revealed a very fine 40-\AA wavelet structure on top of a $300\text{--}500\text{-\AA}$ "pebble grain" texture. In the microscope, crystallization could be induced with the electron beam, and hot-stage examination proved a first crystallization step at $150\text{--}200^\circ\text{C}$. This was confirmed with differential scanning calorimetry where a first crystallization peak (exotherm) at 200°C and two other peaks at higher temperatures were observed.

The smoothed experimental EXAFS data¹² for crystalline and amorphous Ge are shown in Fig. 1. The crystalline data have considerably more detail than the amorphous although the major maxima of both coincide.

Figure 2 shows the result of transforming the smoothed data using Eq. (3). The amplitudes of the two curves are not on an absolute scale since the theory does not calculate an absolute value. They are plotted on slightly different vertical scales for comparison; however, the relative amplitudes of each curve may be compared using

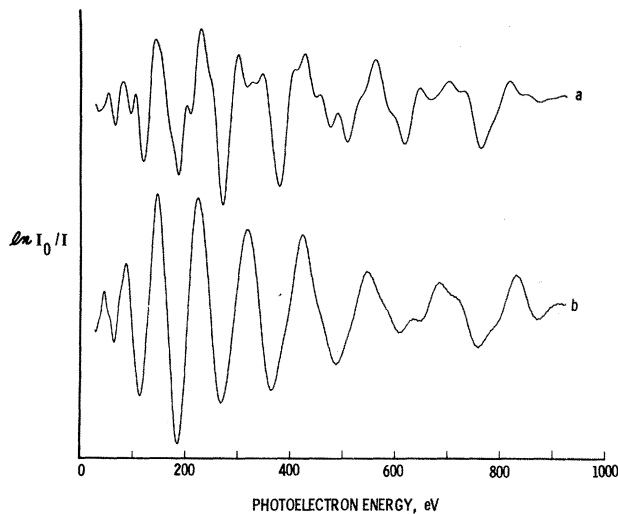


FIG. 1. Smoothed experimental EXAFS data for (a) crystalline and (b) amorphous Ge. Only the oscillatory part χ of the absorption edge is shown.

Eq. (4).

The noted distances to each peak in Fig. 2 are accurate to 1% or better. Note that the distances to the first two amorphous Ge peaks agree exactly with the crystalline distances while any other structure further out is lost in the background. Since the first distance corresponds to the tetrahedral-bond distance and the second distance to the edge of the tetrahedron, this result is compatible with a continuous random network of distorted Ge tetrahedra. The broadened second peak indicates distortion of the bond angle about its crystalline value.

These results differ from earlier results which found that the lattice was expanded $\sim 3\%$ from the crystalline value.¹³ Our results are more in agreement with Moss and Graczyk¹⁴ on Si and the model calculation by Polk.¹⁵ This EXAFS technique is not sensitive to macro- or micro-voids; however, a uniform distribution of atomic-sized vacancies would contribute to the measured values. Micro-voids or larger vacancy clusters were not present since electron diffraction did not show appreciable small-angle scattering. These results confirm those of others^{14,16} who have suggested that the apparent low density in evaporated films is due to the presence of voids not sampled by the density-measuring technique.

Another experimental parameter that can be obtained from the data is γ . If A_j is the experimentally observed amplitude normalized to the

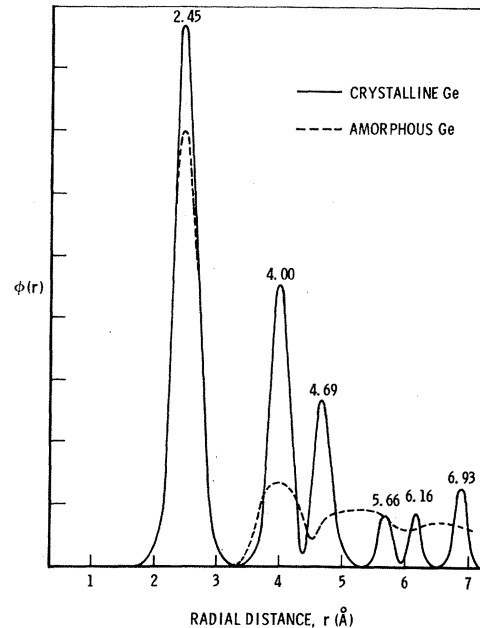


FIG. 2. Fourier transformation of the data of Fig. 1. $\phi(r)$, a radial structure function, compares amorphous and crystalline Ge. Numbers over the peaks indicate the measured distances in \AA .

first peak height, then, from Eq. (4),

$$A_j / (N_j / 2\sigma_j r_j^2) = \exp(-\gamma r_j). \quad (8)$$

For crystalline Ge, N_j and r_j are known and σ_j may be calculated.² A logarithmic plot of Eq. (8) versus r gives a straight line whose slope is $\gamma = 0.31$. This corresponds to a mean free path for scattering into an eigenstate of $1/\gamma = 3.2 \text{ \AA}$. Because this value is small and the near-neighbor structure in amorphous Ge is so similar to that in crystalline Ge, we can assume that the same value of γ applies in both cases. This assumption is important since there is no other way to estimate γ independently and the values of N_j and σ_j which we can determine are sensitive to the choice of γ .

In principle, the amorphous data could be analyzed for N_j and σ_j from the amorphous peak amplitudes and widths with crystalline values for γ and the thermal smearing; however, the present quality of the data is such that the instrumental and Fourier broadening of the peaks overwhelms the expected disorder broadening (0.5 \AA vs about 0.15 \AA) and makes this measurement inaccurate. Work is proceeding to overcome this deficiency. However, comparison of the relative second-shell-peak heights for the crystalline and

amorphous cases gives the result

$$\sigma_D^2(A) \approx 6\sigma_{tot}^2(C). \quad (9)$$

This is a disorder smearing of approximately 0.15 Å meaning that the tetrahedral bonds are distorted $\pm 5^\circ$.

In summary, the point-scattering theory of extended x-ray absorption fine structure can be used, not only to calculate the EXAFS spectrum given the atomic structure, but to invert the experimental data to obtain structural information such as distance, number of atoms, and widths of the coordination shells around a particular atomic species in amorphous materials. Although this technique is still in the developmental stage, our preliminary results on amorphous Ge agree quite well with other recent results and prove that the EXAFS technique is comparable to conventional x-ray or electron scattering methods. The unique feature of this technique is an ability to determine the near-neighbor environment about each different type of atom in a complex material since each atomic x-ray absorption edge occurs at a discrete, easily separable x-ray energy.

*Research supported in part by the Advanced Research Projects Agency of the Department of Defense and monitored by U. S. Army Research Office—Durham under Contract No. DAH CO4 71 C 0010.

†Research supported in part by the U. S. Air Force Office of Scientific Research, Office of Aerospace Research.

‡Presently on sabbatical leave at the Physics Department, Technion, Haifa, Israel. Research supported in part by a National Science Foundation Senior Postdoctoral Fellowship.

¹L. V. Azaroff, *Rev. Mod. Phys.* **35**, 1012 (1963).

²D. E. Sayers, F. W. Lytle, and E. A. Stern, in *Advances in X-ray Analysis*, edited by B. L. Henke, J. B. Newkirk, and G. R. Mallett (Plenum, New York, 1970), Vol. 13, p. 248.

³P. A. Doyle and P. S. Turner, *Acta Crystallogr., Sect. A* **24**, 390 (1968).

⁴T. Shiraiwa, T. Ishimura, and M. Sawada, *J. Phys. Soc. Jap.* **13**, 847 (1958).

⁵R. Kaplow, T. A. Rowe, and B. L. Averbach, *Phys. Rev.* **168**, 1068 (1968).

⁶J. D. Hanawalt, *Z. Phys.* **70**, 293 (1930), and *J. Franklin Inst.* **214**, 569 (1932).

⁷F. W. Lytle, *Developments in Applied Spectroscopy* (Plenum, New York, 1963), Vol. 2, p. 285.

⁸V. V. Schmidt, *Izv. Akad. Nauk. SSSR, Ser. Fiz.* **25**, 977 (1961), and **27**, 384 (1963) [*Bull. Acad. Sci. USSR, Ser. Phys.* **25**, 988 (1961), and **27**, 392 (1963)].

⁹B. E. Warren, *X-Ray Diffraction* (Addison-Wesley, Reading, Mass., 1969), p.127.

¹⁰F. W. Lytle, in *Advances in X-ray Analysis*, edited by G. R. Mallett, M. Fay, and W. M. Mueller (Plenum, New York, 1966), Vol. 9, p. 398.

¹¹R. D. Heidenreich, *Fundamentals of Transmission Electron Microscopy* (Interscience, New York, 1964), p. 45.

¹²We smooth by a band-pass filtering technique which fast Fourier transforms the data into an arbitrary frequency domain and then high- and low-passes this function to remove the low-frequency (slope) and high-frequency (statistical noise) components. The large band-structure maximum at the edge is also removed by this technique.

¹³H. Richter and G. Breitling, *Z. Naturforsch.* **13a**, 988 (1958).

¹⁴S. C. Moss and J. F. Graczyk, in *Proceedings of the Tenth International Conference on the Physics of Semiconductors, Cambridge, Massachusetts, 1970*, edited by S. P. Keller, J. C. Hensel, and F. Stern, CONF-700801 (U. S. AEC Division of Technical Information, Springfield, Va., 1970), pp. 658-662.

¹⁵D. E. Polk, to be published.

¹⁶T. B. Light, *Phys. Rev. Lett.* **22**, 1058 (1969).